# Combined Blade Vibration and Surge/Stall Sensor for Gas Turbine Blade Health Management

**Prof. Kam Chana**

Oxford Thermo-Fluids Institute, Department of Engineering Science, University of Oxford
UNITED KINGDOM

## ABSTRACT

*Turbomachinery blade vibrations is an active area of research. Tip-timing and tip clearance measurements form a major part of turbomachinery health monitoring systems. Currently, non-contact systems such as optical, capacitive, Hall effect, eddy current etc. are used to assess these blade vibrations. However, most of these sensors are prone to contamination, non-linearity and cannot measure both tip-timing and tip-clearance together. Eddy current sensors are found to be robust and can measure both tip-timing and tip-clearance simultaneously using signal processing techniques. Apart from assessing blade vibrations, it will be quite beneficial to predict and prevent surge and stall of compressors in an engine as they can be catastrophic for an aircraft engine during flight. Pressure sensors are generally used to study the variations in the inlet flow for surge and stall protection in an engine and can play an important role in health monitoring.*

*A new combined sensor developed at University of Oxford can measure tip-timing, tip-clearance and dynamic pressure for use in gas turbine engine health monitoring. The combined sensor uses a pressure sensor in the centre and is enclosed by an eddy current sensor forming a compact single package. The pressure sensor used is a fast response optical based sensor that is known to work at high temperatures and is less noisy compared to piezo based pressure sensors. The combined sensor is found to be robust and is able to operate in harsh environments without any loss in accuracy. Due to the combined package, the space occupied is much less compared to that required by two separate sensors. The sensor has many applications that include measuring vibrations, active flow control, stall/surge of compressors etc.*

*The paper presents the design and development of this combined sensor along with some experimental results on tip timing and unsteady pressures from a gas turbine engine fan blades. The engine tests included looking at the effect of distorting the inlet flow on blade vibrations by placing varying number of bars in the inlet duct of the engine.*

## 1.0   INTRODUCTION

Timely maintenance of gas turbine components is achieved through active health monitoring systems. The vibrations of blades in a gas turbine engine are caused by dynamic loading due to rotor imbalances, varying blade tip clearance due to non-concentric casings and distortions in the inlet flow (caused by irregular intake geometries). These can cause high cycle fatigue and hence damage the blades. This will potentially have a significant impact on the safety and whole life costs of the engine. Detection of the changes in blade vibration modes and levels due to damage or deterioration would allow improvements to the inspection, repair and replacement process.

Methods used to measure Blade Tip-Timing (BTT) and tip-clearance generally involves the use of optical probes, eddy current, capacitive, Hall effect sensors etc. [1], [2], [3], [4]. All these sensors measure the arrival time of the blades and some can measure the tip-clearance (eddy current and capacitance). Among these sensors the eddy current sensor is robust and immune to contaminations [5].

To measure surge and stall of compressors, pressure sensors are used to look at the variations in the inlet flow. The aim of this research is to show the performance and accuracy of a newly developed combined pressure and eddy current sensor and its application in measuring tip-timing and inlet flow disturbances in the fan stage of a small gas turbine engine.

## 2.0 IMPROVED EDDY CURRENT SENSOR

A normal off the shelf eddy current sensor generally contains a circular coil, however these tend to lose resolution and accuracy when encountering blade vibrations due to the blade profile. Elongated coils on the other hand are better suited for blade vibration applications as the coil generates a directional field and can be easily aligned with the blade profile as shown in figure 1a. This helps in detecting vibrations of the blades accurately. The sensor generally has a range of half its diameter.
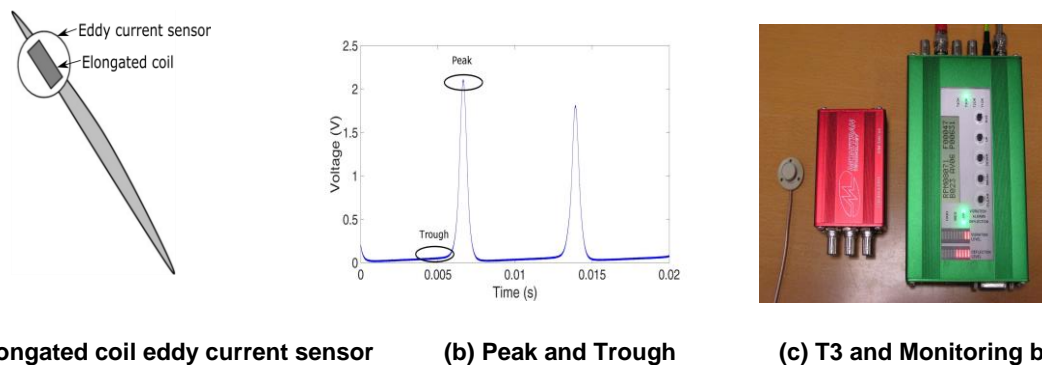


|          (a) Elongated coil eddy current sensor          |          (b) Peak and Trough          |          (c) T3 and Monitoring box          |

**Figure 1: Eddy current sensor and electronics**

Apart from the improvements in the sensor design, the signal from the sensor needs to be processed accurately to extract the blade arrival time and clearance information. A peak-and-trough method [6] is used to calculate the inter blade time of arrival. The algorithm takes 50 percent value of the voltage difference between the preceding trough and the current peak and the temporal position at which this value occurs on the falling part of the curve gives the inter blade time of arrival (figure 1b). This is done to avoid digital data storage and streamline the electronics that is small and consumes low power for on-wing applications.

The eddy current sensor interfaces to a signal conditioning electronics box called the turbine-tip-timing unit (T3) (Fig. 1c). The T3 box drives the probe with an oscillating frequency of about 1MHz and also processes the signal in a manner where the tip clearance is separated from the blade arrival time information. The T3 outputs the time of arrival trigger pulse, the raw eddy current sensor signal, and scaled tip clearance. The T3 output is then used with an off the shelf tip-timing system or a bespoke DSP system for health monitoring.

## 3.0 EDDY CURRENT SENSOR SYSTEM VALIDATION AGAINST OPTICAL SYSTEM

The T3 and eddy current sensor comparison was carried out in conjunction with Rolls Royce Derby against an optical sensor (XP84049). Four eddy current and optical sensors were installed on the first and second stage fan rotors a Spey engine as shown in figure 2. On each stage the probes were arranged to be over the leading edge of the rotor, at the same axial position as the centre of the eddy current sensors, but separated by a circumferential distance. All the optical probes were routed to a nearby cabin where they were connected to an optical conditioning box for the laser transmission and receive signals. The optical probe conditioning laser brick provides

illuminationinto one half of the bifurcated fiber optic, which is transmitted to, and emitted from the tip of the probe. As the blades on the rotor under test pass the probe, some light is reflected back into the probe, and is transmitted into the other half of the fiber bundle to a detector.
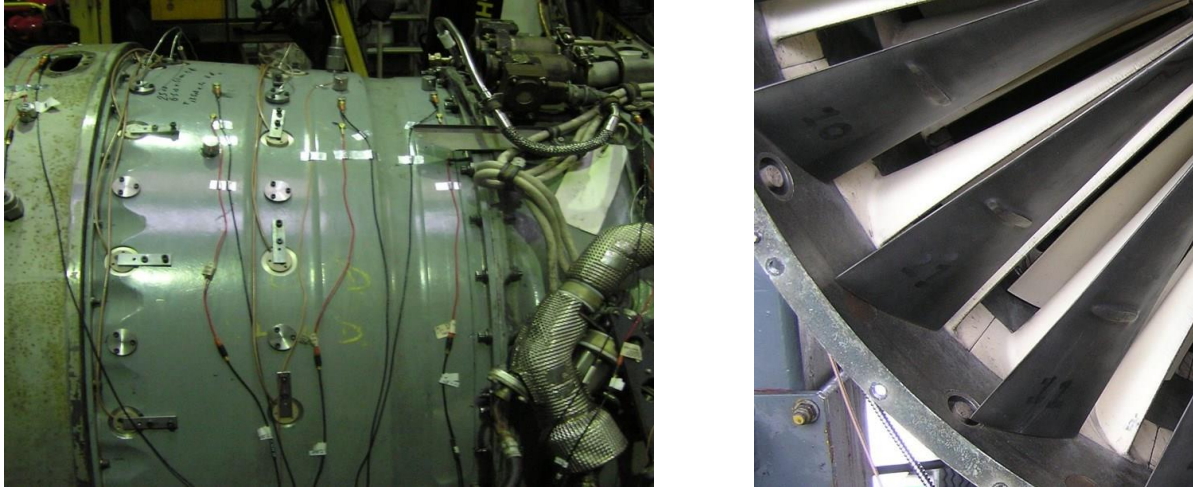


**(a) External view of sensor installation on Spey engine**

**(b) Internal view of sensor installation on Spey engine**

**Figure 2: Sensors on Spey engine**

Figure 3 shows the time of arrival for each blade. The engine run (top graph of the Fig. 3) consists of idling for few minutes and throttling up and maintaining full speed for a couple of minutes and then decelerating back to idle. We note that as the RPM increases, the time of arrival between the blades decreases. Excellent agreement was achieved using directional eddy current sensors and the new triggering technique. The eddy current sensor showed excellent contamination resistance compared to optical probes when the engine was operated in rainy conditions (fourth graph in Fig. 3) showing its application for in-flight measurements. Further details about the sensor development validation is described in ASME papers [5] and [7].

## 4.0   COMBINED EDDY CURRENT AND PRESSURE SENSOR

The combined eddy current and pressure sensor is a new concept that tested on a gas turbine engine. The idea behind the sensor is that it provides two different technologies to detect the onset of an issue and hence reduce
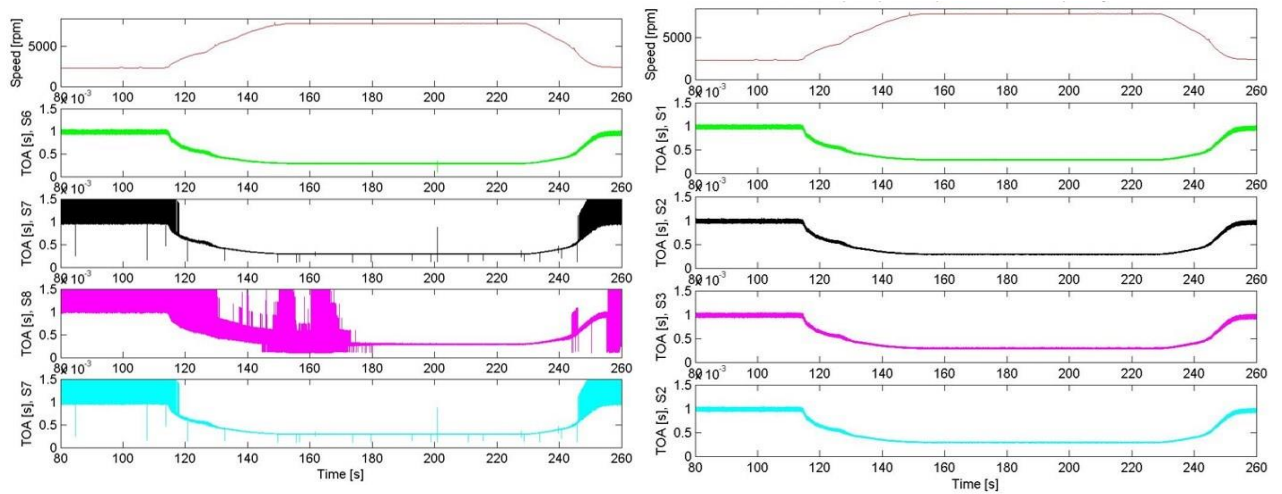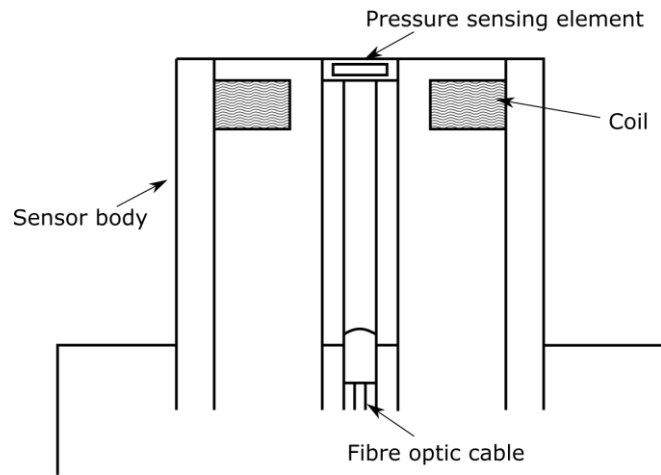
(a) Optical sensor  (b) Eddy current sensor

Figure 3: Time of arrival comparison between optical and eddy current
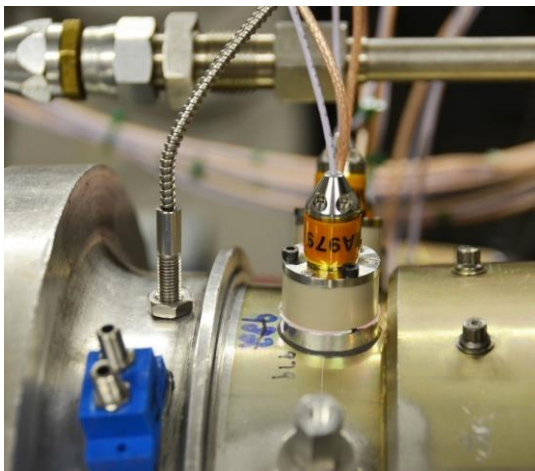


(a) Combined sensor  (b) Schematic of combined sensor

Figure 4: Combined sensor

**Figure 5: Oxsensis driver (PT2400™)**

the likelihood of false alarms. Since the sensor has dual use, the need for extra mounting for another sensor is no longer required.

For the dynamic pressure part of the probe, the signal is transmitted via a standard fibre optic cable to an Oxsensis [R] signal conditioning unit that combines all of the optical components with the required electronics to produce a calibrated pressure output (Fig. 5). The output from the box is fed to a 16-bit National Instruments high speed data acquisition (DAQ) card. The data was sampled at 1mega samples per second (MSPS) per channel. The probe cable was extended using standard 12m fibre extension cables to reach the control room where the electronics were situated. The 12m fibre extensions did not degrade the signal quality.

## 5.0 ENGINE TEST

Six probes were fitted to the casing of the fan over the first stage fan blade as shown in figure 6a. Figure 6b shows the sensor locations around the casing from the top dead centre position. Probe 1 was located at 245° and Probe 6 at 0°. Probes 3 and 4 were not forward as the casing squeeze mechanism bars prevented these probes from being fitted at a more forward location.

### 5.1 Inlet Distortion of Flow

The inlet aerodynamic distortion tests were performed by introducing a set of 19 aerofoil shaped bars fitted in the inlet duct of the engine upstream of the fan blade row (Fig. 7a). They were thicker at the rear in order to generate wakes. Figure 7b shows the engine fitted with the 19 bar ring. The rings consist of a hub and casing circular ring interconnected with a series of bars that are profiled in shape.
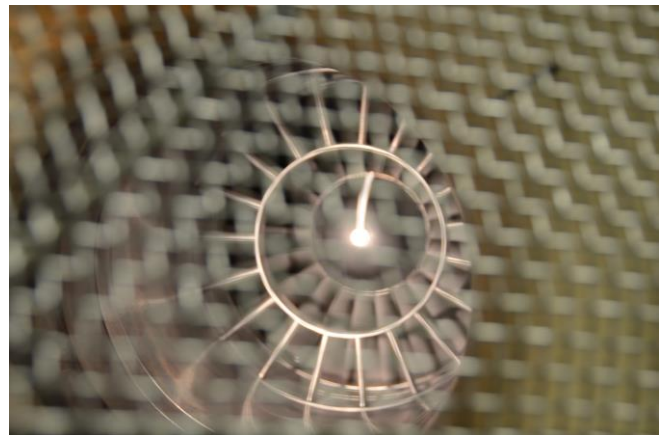
(a) Sensor on the engine
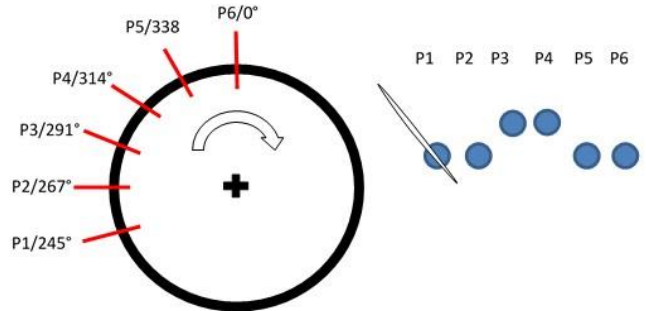


(b) Locations of the sensors on the engine

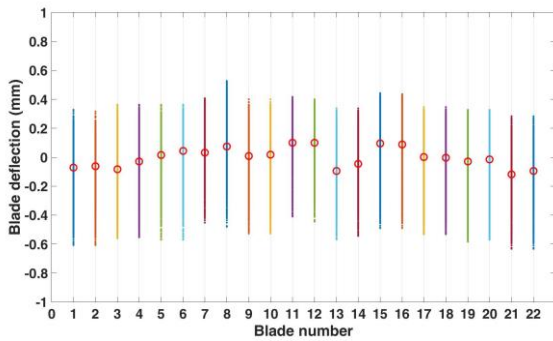**Figure 6: Combined sensor and mounting**
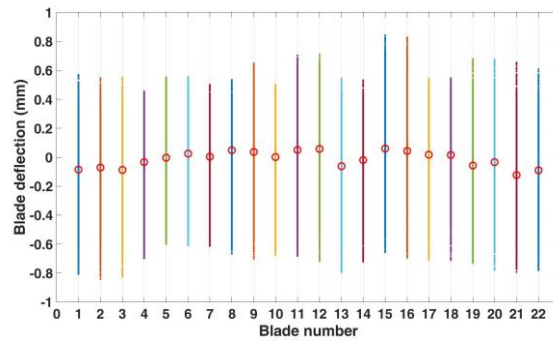


(a) Bars used in the experiments for inlet distortion



(b) Engine inlet with bars in the front

**Figure 7: Engine inlet with bars**



(a) No bars



(b) 19 bars

**Figure 8: Deflections with and without bars**
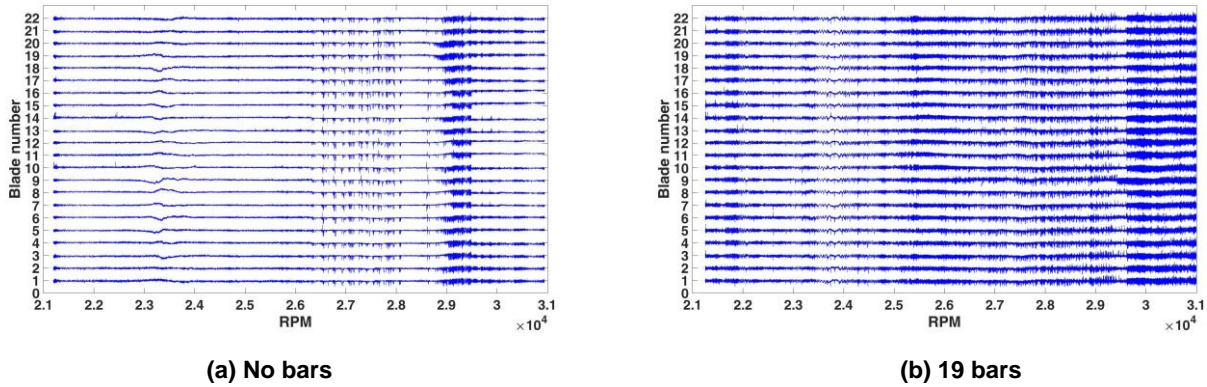
(a) No bars            (b) 19 bars

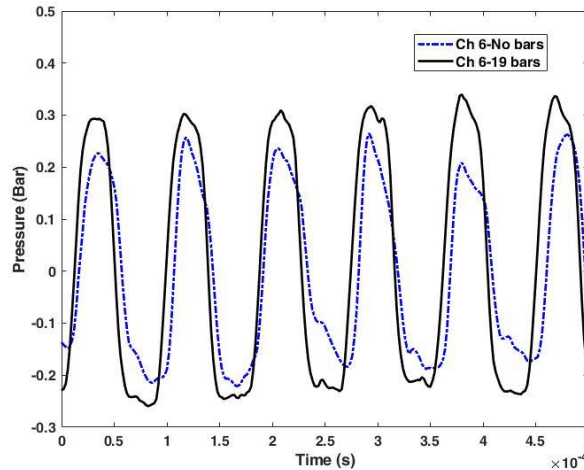**Figure 9: Waterfall plots with and without bars**



**Figure 10: Pressure with and without bars**

Figure 8 shows the blade tip deflection for each blade in every revolution and an average over the run duration. The results processed for this data are taken during the acceleration part of the engine run. Notably the blade tip deflection for the uniform inlet without distortion (Fig. 8a) shows a significantly smaller blade tip deflection range in comparison to the results with the inlet distortions compared to 19 bars (Fig. 8b).

Using the tip timing data, a waterfall plot is created showing each blade on the y-axis and engine speed on the x-axis (Fig. 9). The blade deflection is scaled and shown in the vertical plane for each blade trace. As the engine is accelerated from idle to full operating speed, the points at which the blade experiences a resonance can be easily seen using this type of plot. Figure 9a shows the results for the uniform inlet case where there is no inlet distortion introduced. After 23,000 rpm, all blades experience a resonance which seems to be the blade or rotating assembly's natural resonance that is usually linked to blade flutter. At around 26,500 rpm the blades experience a further resonance until around 28,000 rpm. The largest resonance is noted at just before 29,000 rpm which ends at around 29,500 rpm.

Similar waterfall plot for 19 bars (Fig. 9b), shows the resonance increases significantly. An interesting point to note is the resonance occurring at 23000 RPM in the case of no bars shifts to ≈ 24000 RPM for 19 bars. This can be due to the fact that the unsteady wake flow at inlet produced by the bars resonates with the fan over the RPM range of the engine leading to large deflections. Further details about the testing are published in ASME paper [8]

Figure 10 shows the unsteady casing pressures for the uniform undisturbed inlet, 19 bars inlet distortion from the combined pressure and tip timing probe 6. The amplitude of the unsteady pressure levels are larger for the case with 19 bars compared with no bars as expected.

## 6.0   TIP TIMING USING INTEGRATION METHOD

The peak and trough method was successfully implemented in the field with more than 200 units operating for over 10 years at various power stations. It was found that the accuracy can be further improved using better algorithms. A new method based on integration [9] was developed which identifies two points (Fig. 11) on the curve's rising and falling side that exceeds the threshold voltage for each signal from a blade and calculates the area under the curve using the trapezoidal rule which is given by equation 1.

$$\int_a^b f(x)dx \approx \frac{b-a}{2N} \sum_{n=1}^{N} (f(x_n) + f(x_{n+1}))$$

(1)

Once the area is calculated for a curve, the temporal position where the area of curve reaches 50% the value of the curve in the next revolution is calculated. This temporal position will be the inter blade time of arrival for that blade. An advantage of this method is that the noise is symmetric throughout and while integrating, the noise is averaged out.

Figure 12 shows the time of arrival comparison between the peak-and-trough and integration method. We note that the variation of arrival time in integration method (0.0000248s) is significantly less than the peak-and-trough method (0.0000329s) as the noise that affects the inter blade time of arrival evaluation is significantly reduced by the integration method. From these comparisons, we can justify that the integration method performs significantly better than the previous method in the presence of noise.
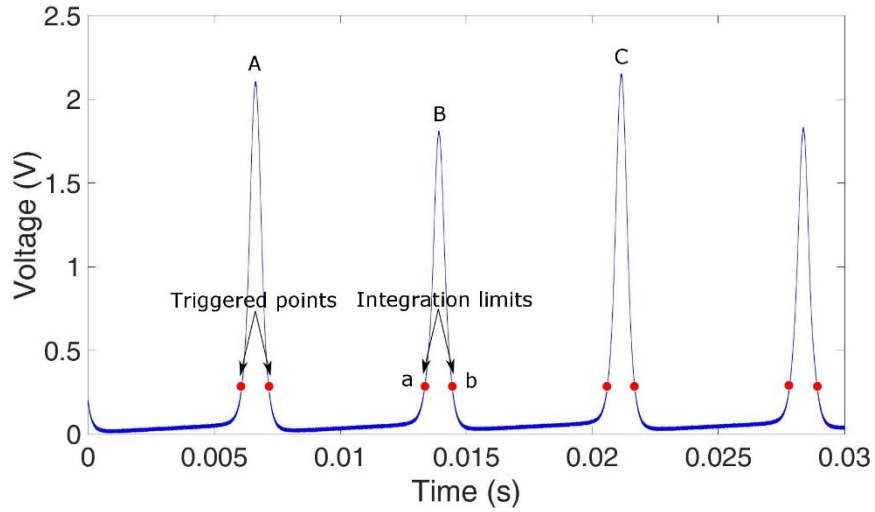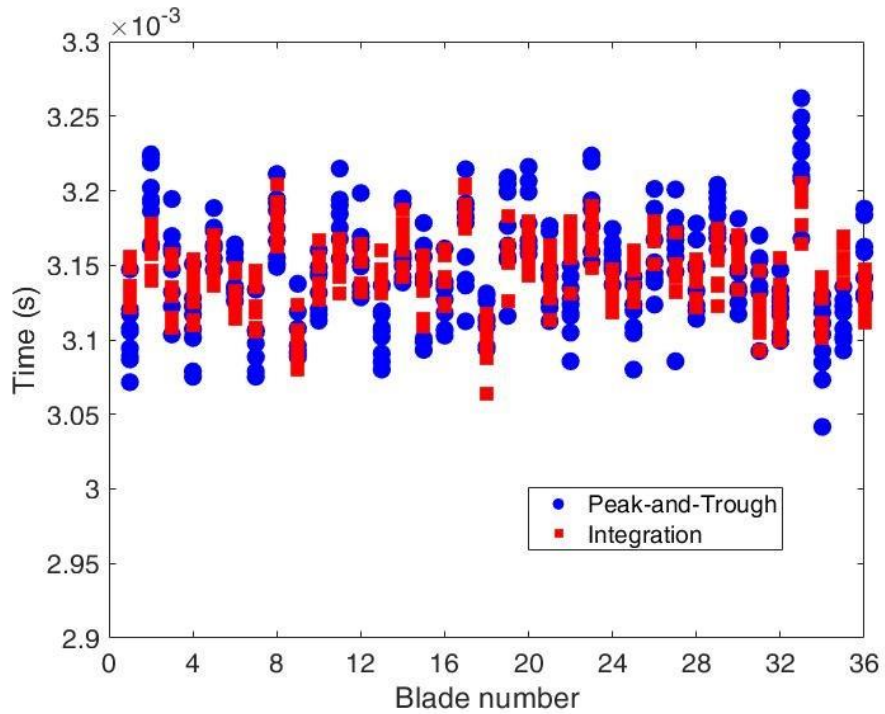
**Figure 11: Data showing the integration limits**



**Figure 12: 36 Blade at 530 RPM**

## 7.0   DSP AND DASHBOARD



**Figure 13: DSP and driver electronics**

With all the previous off and on site testing with eddy current sensors, driving electronics and signal processing algorithms a compact electronics driver is built and the algorithms to process tip timing and clearance are incorporated into a digital signal processor (DSP) (Fig. 13). The system now has the capability to process up to 12 inputs and can monitor multiple engines in real time. The processed data and results can be transmitted to a wide range of interface mediums; for example to a dedicated PC, to specific engine control systems software or, via an ethernet link, to a web based application accessible anywhere in the world. Real time and in-service availability of performance data on dashboards continuous data provision allows trends to be identified and monitored for scientifically-informed, proactive, preventative decision-making. The technology has proven reliability with 200+ eddy current sensors currently in service on industrial turbines worldwide and with bespoke customer dashboard configuration that pinpoints preventative maintenance opportunities ensuring long service life, low maintenance cost, optimise uptime, minimise risk and enhance productivity.

## 8.0   EXPLOITATION MATURITY METRICS

Table 1 shows the exploitation maturity metrics or exploitation maturity level (EML) neatly proposed by the UK MOD. The levels start from zero where there is no end user identified to level 6 where an end user is identified and is actively using the technology in relevant area. When this EML is used against the standard technology readiness level, we get a matrix as shown in table 2 that shows where the current technology lies. For example, a technology can be at a high TRL but has not been matured with an end user for in-service.

**Table 1: Exploitation maturity metrics**

| EML | EML Description - For Use in UK MOD Health and Usage technology maturation | Summary |
|---|---|---|
| 0 | No end user/operator or industry OEM exploiter has been identified | Low |
| 1 | The proposer has aspirations for the results of the offering to be exploited by an identified end user/operator or industry OEM exploiter has been identified | |
| 2 | The proposer has involved an identified end user/operator or industry OEM in preliminary discussions about the offering and its applicability | |
| 3 | The proposer has liaised withan identified end user/operator or industry OEM and they have produced and agreed an exploitation plan | Medium |
| 4 | An identified end user/operator or industry OEM is actively supporting or is involved in the successful exploitation of the offering | |
| 5 | An identified end user/operator or industry OEM has a formal commitment to use the results of the offering subject to meeting agreed TRL level | High |
| 6 | An identified end user/operator or industry OEM is actively using the results of the research in a relevant area | |

**Table 2: TRL v/s EML matrix**

**Table 3: TRL v/s EML for Tip timing and clearance for industrial applications**

| | Lab based tests and ID of potential development partners | Proof of concept on real engines | Sensor performance validation and optimisation | Accelerated Life Testing/ Certification Issues | In-Flight Tip Clearance / timing Systems | |
|---|---|---|---|---|---|---|
| Sensor concept developer | Prototype sensor signal conditioning design performance tests DSP Design | Proof of concept tests Concept of employment Analysis suite development | Performance assessment/ optimisation Actionable Condition Indicators (ACI) | Future Developments E.g. Improved sensitivity | Future Developments E.g. multi-parameter sensors | EML Low |
| Sensor Supplier | Commercial, IP and legal arrangements | Hot and cold functional tests Vibration and thermal integrity tests | Manufacture sensors Manufacture DSP Software for ACI logging/analysis | Manufacture & Sensor Certification | Supply Industrial sensor, signal conditioning unit and DSP to OEMs | EML Medium |
| OEMs | Tip timing requirements ID and provide test platform | Test platform sensor system and engine integration | Final sensor design Identify target platform for sensor system | Provide target platform for in-service tests | In-service use and supported | EML High |
| | TRL 2-3 | TRL 3-4 | TRL 5-6 | TRL 6-7 | TRL 7-8 | |
| 2010 | | | | | 2018 | |

**Table 4: TRL v/s EML for Tip timing and clearance for aerospace applications**

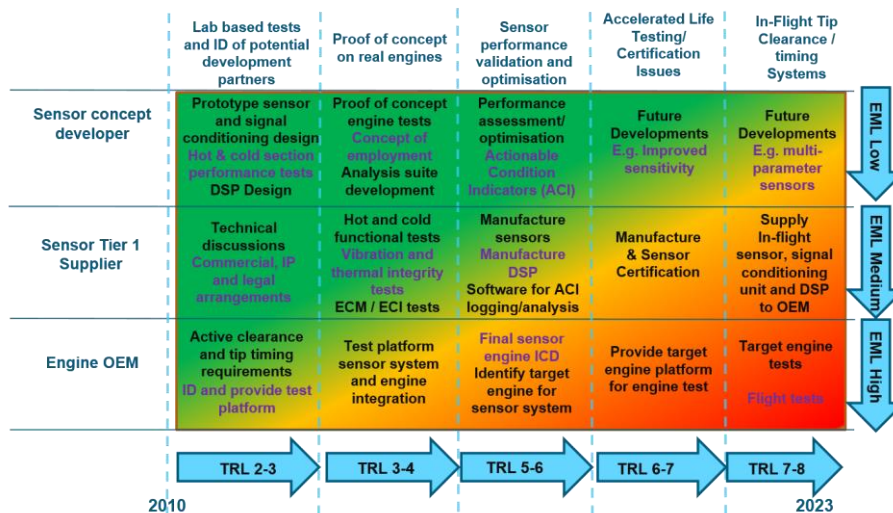| | Lab based tests and ID of potential development partners | Proof of concept on real engines | Sensor performance validation and optimisation | Accelerated Life Testing/ Certification Issues | In-Flight Tip Clearance / timing Systems | |
|---|---|---|---|---|---|---|
| Sensor concept developer | Prototype sensor and signal conditioning design Hot & cold section performance tests DSP Design | Proof of concept engine tests Concept of employment Analysis suite development | Performance assessment/ optimisation Actionable Condition Indicators (ACI) | Future Developments E.g. Improved sensitivity | Future Developments E.g. multi-parameter sensors | EML Low |
| Sensor Tier 1 Supplier | Technical discussions Commercial, IP and legal arrangements | Hot and cold functional tests Vibration and thermal integrity tests ECM / ECI tests | Manufacture sensors Manufacture DSP Software for ACI logging/analysis | Manufacture & Sensor Certification | Supply In-flight sensor, signal conditioning unit and DSP to OEM | EML Medium |
| Engine OEM | Active clearance and tip timing requirements ID and provide test platform | Test platform sensor system and engine integration | Final sensor engine ICD Identify target engine for sensor system | Provide target engine platform for engine test | Target engine tests Flight tests | EML High |
| | TRL 2-3 | TRL 3-4 | TRL 5-6 | TRL 6-7 | TRL 7-8 | |
| 2010 | | | | | 2023 | |

Table 3 shows the TRL v/s EML matrix for tip timing sensors used in the larger gas turbine found within the power generation industry. The technology has been fully developed and exploited with industrial partners. This explains why the TRL/EML matrix in table 3 is all green. It is already being used to monitor industrial steam and gas turbines for power generation with large OEMs.

The technology however is still being developed with aerospace engine OEMs to enhance the TRL and EML (see table 4). Significant testing is being carried out in-house, OEMs and other research laboratories. The technology is exploited through a licensing agreement with Proxisense [R] who are streamlining the manufacturing process and developing it through collaborations with OEMs for aerospace applications. At the current pace the technology is expected to reach TRL 7/8 and EML 6 by end of 2023, where it will be exploited for aerospace applications.

## 9.0 CONCLUSIONS

The paper shows that the eddy current sensors along with novel algorithms and electronics perform significantly better than the optical sensors under various test conditions both in-house and on developmental engine test beds. The sensor is clearly able to detect the variations in blade vibrations caused due to aerodynamic forcing. The combined sensor can be used to predict surge and stall of an engine as well in the same package thus reducing the weight and structural modifications to the engine.

## 10.0 ACKNOWLEDGEMENT

## 11.0 REFERENCES

[1] Flotow, A.V., Mercadal, M., and Tappert, P., "Health Monitoring and Prognostics of Blades and Disks with Blade Tip Sensors," Proceedings of IEEE Aerospace Conference, Vol. 6, 2000, pp. 433–440.

[2] Lattime, S.B. and Steinetz, B.M., "Turbine Engine Clearance Control Systems: Current Practices and Future Directions," 38th Joint Propulsion Conference and Exhibit cosponsored by AIAA, ASME, SAE, and 47th AIAA Aerospace Sciences Meeting Including The New Horizons Forum and Aerospace Exposition, No. NASA NASA/TM–2002-211794 AIAA-2002-3790, Orlando, Florida, 2009.

[3] Vakhtin, A.B., Chen, S., and Massick, S.M., "Optical Probe for Monitoring Blade Tip Clearance," 47th AIAA Aerospace Sciences Meeting Including The New Horizons Forum and Aerospace Exposition, No. 2009-507, Orlando, Florida, 2009.

[4] Hafner, M., Holst, T., and Billington, S., "Blade Tip Measurement Advanced Visualization using a Three dimensional representation," ASME 2011 Turbo Expo: Turbine Technical Conference and Exposition, No. GT2011-46523, Vancouver, Canada, 2011, pp. 419–425.

[5] Chana, K.S., Cardwell, D.N., and Russhard, P., "The Use of Eddy Current Sensors for the Measurement of Rotor Blade Tip Timing Sensor Development and Engine Testing," Proceedings of the ASME Turbo Expo 2008: Power for Land, Sea and Air, No. GT2008-50791, 2008.

[6] Chana, K.S., "Eddy Current Sensors," Patent No. CA2688645A1, 2009.

[7] Chana, K.S. and Cardwell, D.N., "The Use of Eddy Current Sensor Based Blade Tip Timing for FOD Detection," Proceeding of the ASME Turbo Expo 2008: Power for Land, Sea and Air, No. GT2008-50792, 2008.

[8] Sridhar, V. and Chana, K., "Development of a combined eddy current and pressure sensor for gast turbine blade health monitoring," Proceedings of ASME Turbo Expo 2017, No. GT2017-63807, ASME, June 2017, pp. 1–8.

[9] Chana, K.S., Sridhar, V., and Singh, D., "THE USE OF EDDY CURRENT SENSORS FOR THE MEASUREMENT OF ROTOR BLADE TIP TIMING: DEVELOPMENT OF A NEW METHOD BASED ON

[10] INTEGRATION," Proceedings of ASME Turbo Expo 2016, No. GT2016-57368, ASME, ASME, June 2016, pp. 1–8.